ACS Sustainable Chemistry & Engineering

pubs.acs.org/journal/ascecg

Research Article

# Influence of Carbohydrates Covalently Bonded with Lignin on Solvent Fractionation, Thermal Properties, and Nanoparticle Formation of Lignin

Rui Liu, Annika Smeds, Teija Tirri, Hongbo Zhang, Stefan Willför, and Chunlin Xu*

Cite This: *ACS Sustainable Chem. Eng.* 2022, 10, 14588−14599

Read Online

ACCESS | Metrics & More | Article Recommendations | Supporting Information

**ABSTRACT:** The valorization of industrial lignin essentially requires fractionation resulting in lower structural heterogeneity and polydispersity. So far, extensive fractionation approaches based on extraction with solvents, gradient acid precipitation, and membrane-based filtration have been developed to reduce the polydispersity and heterogeneity of technical lignins. However, most reports tend to overlook the lignin fraction that bonded with carbohydrates or the so-called lignin carbohydrate complex (LCC), which always coexists in the initial lignin sample and can significantly affect the properties of lignin, including its homogeneity and solubility. In this study, we evaluated the ability of 13 organic solvents to separate lignin bonded with carbohydrates. It was found that carbohydrates could only be detected when the hydrogen bonding capacity ($\delta$H) of solvent was no less than 8.0 (the $\delta$H of tetrahydrofuran, THF). Based on this result, eight lignin fractions with trace/large amounts of carbohydrates and decreased heterogeneity were obtained using an elaborate sequential solvent extraction approach. The following properties of each lignin fraction were compared: elemental composition, carbohydrate content, molar mass, hydroxyl group content, and thermal properties. In addition, we also studied the ability of these lignin fractions to form lignin nanoparticles and confirmed that fractions with trace amounts of carbohydrates were able to form uniform spherical lignin nanoparticles (LNPs) than those with large amounts of carbohydrates bonded fractions. In short, this study provided a profound understanding of the role of the carbohydrates bonded to lignin on the fractionation of lignin by organic solvents, further demonstrating how carbohydrates influence the characteristics of lignin.

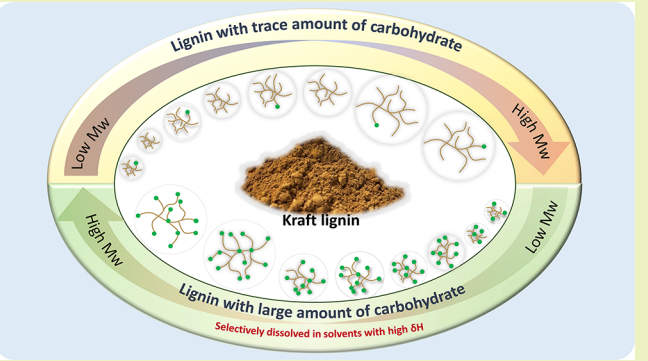


**KEYWORDS:** *softwood kraft lignin, solvent fractionation, lignin carbohydrate complex, thermal properties, lignin nanoparticles*



## INTRODUCTION

Lignin is the most abundant aromatic polymer derived from wood and nonwood plants. It is acknowledged as a highly heterogeneous polymer consisting of three different monomeric units (C3−C6 units), namely, *p*-coumaryl alcohols, coniferyl alcohol, and sinapyl alcohol, which are disorderly bonded together within the enzymes-mediated dehydrogenation/radical coupling reaction in plants.[1−3] Lignin macromolecules have several characteristic functional groups: phenolic and aliphatic hydroxyls, carboxylic, methoxy, and carbonyl groups, which offer enormous potential for chemical modifications and thereby facilitate the valorization of lignin in various fields.[4] So far, a great deal of research has been devoted to developing ways of lignin utilization, for example, to converting lignin into phenolic compounds using catalytic approaches,[5] to preparing lignin-derived copolymer materials,[6,7] and to exploring its potential in the biomedical field, such as in the subfield of antibacterial materials,[8,9] nanomedicine,[10−12] tissue engineering,[13,14] and so on.

However, the valorization of lignin is still limited due to the lack of well-refined lignin sources, even though millions of tons of lignin, the byproduct of industrial lignin to be precise, are annually retrieved from wood in pulp and paper manufacturing and other biorefinery processes.[15] The reason could be that the structure of lignin is not only extremely complex and diverse in its native state but that it can also be profoundly changed when different chemical delignification methods are used during the pulping or biorefinery processes.[16] On the other hand, the industrial lignins are always complex mixtures containing various components: chemical residues, nonlignin relevant substances from wood extractives, numerous degradation

Received: July 30, 2022
Revised: October 7, 2022
Published: October 24, 2022

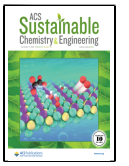

products, and especially the variable content of carbohydrates covalently bonded with lignin, which could result in significant discrepancies in the physicochemical properties of lignin and then consequently influence its behavior in downstream applications. For example, it was reported that the carbohydrates covalently bonded to lignin could seriously affect it solubility in solvents.[17] Moreover, it was also reported that the needed concentration of lignin with carbohydrates to inhibit 50% of chondrocyte cell (IC50) was higher than the required concentration of lignin almost free of carbohydrates, which suggested a difference in biocompatibility among lignin fractions with or without carbohydrates.[18] Thus, the potential differences between lignin and carbohydrate covalently bonded lignin (or the so-called lignin carbohydrate complex, LCC) should be seriously considered regardless of the lignin fractionation and applications.

The transformation of industrial lignin into a value-added material by fractionation has been carried out for a long time. One of the current research goals is to fractionate lignin components that are controllable in terms of their molecular distribution, as well as the abundance of different functional groups and interunit bonds.[15] Up to now, the prevalent approaches for the fractionation of industrial lignin have usually depended on solvent extraction including single solvent and sequential solvent extraction, selective acid precipitation at reduced pH values, and membrane ultrafiltration.[15] Using these methods, lignin fractions with a narrow molar mass can be targeted; however, the coexistence of complicated and varying LCC in both molar mass and total content makes controlling the quality of lignin challenging. Therefore, successful separation of lignin with/without carbohydrates is meaningful both for decreasing the heterogeneity of lignin and for facilitating lignin applications according to its structural characteristics.

Studies done on the dissolution of lignin in organic solvents have revealed interesting dissolution behaviors for lignin. By identifying the solubility of lignin in various organic solvents, Schuerch has concluded that solvents with a considerable hydrogen bonding capacity or basic strength can increase the dissolution of lignin fraction with higher molar mass.[3] For example, dioxane always showed better performance than acetone and ethers in dissolving various lignins.[3] In addition, experiments have also proven that the solubility of lignin could increase gradually with decreasing hydrocarbon chain length in homologous alcohols.[19−21] Moreover, in order to understand the potential influence of solvents on lignin dissolution, and to look for a rational solvent sequence to perform lignin fractionation, the solubility parameter theory of Hildebrand and the Hansen solubility parameter (HSP) have been employed to study the potential relationship between lignin solubility and common industrial solvents, which provided both experimental and theoretical directions for lignin fractionation.[20] According to Hildebrand theories, it was reported that the solubility parameter of lignin is in the range 12−28 $(cal/cm^3)^{1/2}$ depending on the lignin sources and pulping process.[22] However, the Hildebrand solubility parameter was inapplicable for polar solvents; thus, the HSP theory ($\delta^2 = \delta^2D + \delta^2P + \delta^2H$) relating to dispersion forces ($\delta D$), polar interactions ($\delta P$), and hydrogen bonding ($\delta H$) was proposed for studying the correlation between lignin solubility and solvent properties.[20,23] However, although it was reported that ambiguous types and quantities of carbohydrates that are covalently bonded to lignin would greatly affect the solubility of lignin in organic solvents,[17,24,25] the potential effect of carbohydrates covalently bonded with lignin on its dissolution in various organic solvents was usually overlooked in earlier studies,[19,20] where the theories of Hildebrand and Hansen solubility parameter were employed.

In a previous study,[26] we carried out the sequential extraction by the solvent order of methyl *tert*-butyl ether (MTBE), ethyl acetate (EtOAc), ethanol (EtOH), methanol (MeOH), acetone (dimethyl ketone, DMK), and dioxane to study the component characteristics of industrial softwood kraft lignin. One interesting finding was that the obvious carbohydrate signals were only detected from the fractions extracted by EtOH, MeOH, and dioxane, which are solvents with a higher hydrogen bonding ability. This result indicated that the solubility of lignin with trace/larger amounts of covalently bonded carbohydrates varies significantly in solvents with different hydrogen bonding abilities. In other words, it would be possible to separate lignin without LCC contamination by controlling the solvent hydrogen bonding ability. To verify this hypothesis, in this study, we preliminarily compared the carbohydrate content of lignin fractions that were extracted alone by several commonly used organic solvents in lignin chemistry. Whereafter, a new solvent sequence is proposed to separate narrow molar mass lignin fractions with trace/large amounts of carbohydrates. We also discuss the characteristics variation of lignin in the thermal properties and in the formation of lignin nanoparticles.

## MATERIALS AND EXPERIMENT

Softwood Kraft lignin (KL) powder (UPM BioPiva 350) was obtained from UPM FOREST (Finland). According to our previous study,[26] this kind of technical grade lignin contains plenty of impurities, such as wood extractives, carbohydrates, inorganics, and polysulfide. Therefore, the lignin sample was first purified with acidic water (pH, 2.5) and then repeatedly extracted by methyl *tert*-butyl ether (MTBE) until no extractive signals, such as resin acids and fatty acids, could be detected by gas chromatography−mass spectrometry (GC−MS) from the concentrated MTBE solution.

**Solvent Screening.** Thirteen organic solvents, dimethyl sulfoxide (DMSO), *N*,*N*,-dimethylformamide (DMF), dioxane, tetrahydrofuran (THF), pyridine, acetone, MeOH, EtOH, EtOAc, isopropanol, dichloromethane (DCM), diethyl ether, and hexane (all in HPLC grade) were used to carry out a single-solvent extraction. In general, 300 mg of prepurified lignin was added to a 15 mL centrifuge tube, and then, lignin was extracted with a moderate volume of the mentioned solvents repeatedly by mechanical shaking until an almost colorless supernatant was finally obtained. The liquid supernatant of each solvent was collected and combined after a solid−liquid separation by centrifugation at a speed of 12 500 rcf for 5 min. Note, the lignin needed to be dispersed well by vortex or ultrasound during each repetition, and the final residue was dried and weighted for the calculation of fractionation yield. Due to the different boiling points of each solvent, the fractions were concentrated by a rotary evaporation and then dried in a vacuum oven or to remove solvents by dialysis (DMF and DMSO only) in distilled water through a regenerated cellulose dialysis membrane with a molar mass cutoff of of 1000 Da. The lignin dispersed in the dialysis membrane was collected and freeze-dried and then dried by a freeze-dryer. The carbohydrate in each fraction was qualitatively analyzed by the acid methanolysis method and determined with a gas chromatograph combined with a flame ionization detector (GC-FID).

**Sequential Extraction of Lignin.** Based on the results of solvent screening, DMK, EtOH, MeOH, EtOAc, and THF were used for sequential lignin fractionation. First, 10 g of prepurified and dried KL were first extracted by DMK repeatedly and until an almost colorless liquid finally presented to separate lignin fraction with a trace amount


https://doi.org/10.1021/acssuschemeng.2c04498
ACS Sustainable Chem. Eng. 2022, 10, 14588−14599

Table 1. Properties of Organic Solvents, the Extraction Yield of Each Solvent, and the Carbohydrate Content[a]

| | Hanson solubility parameter[23] | | | | | | | | |
|---|---|---|---|---|---|---|---|---|---|
| solvent | δD ($MPa^{1/2}$) | δP ($MPa^{1/2}$) | δH ($MPa^{1/2}$) | molar volume[23] $cm^3\ mol^{-1}$ | Hildebrand solubility parameters[33] ($MPa^{1/2}$) | ε[34] (293.2k) | $b_p$[34] (°C) | yield (wt%) | carbohydrates content |
| DMSO | 18.4 | 16.4 | 10.2 | 71.3 | 24.5 | 47.24 | 189 | 96% | + |
| DMF | 17.4 | 13.7 | 17.4 | 77.4 | 24.1 | 38.25 | 153 | 95% | + |
| dioxane | 17.5 | 1.8 | 9.0 | 85.7 | 20.7 | 2.22 | 101.5 | 85% | + |
| THF | 16.8 | 5.7 | 8.0 | 81.7 | 18.6 | 7.52[b] | 65 | 82% | + |
| pyridine | 19.8 | 8.8 | 5.9 | 80.9 | 21.7 | 13.26 | 115.23 | 83% | + |
| DMK | 15.5 | 10.4 | 5.7 | 74 | 19.6 | 20.1 | 56.05 | 67% | − |
| MeOH | 14.7 | 12.3 | 22.3 | 40.7 | 29.7 | 32.6 | 64.6 | 55% | + |
| EtOH | 15.8 | 8.8 | 19.4 | 58.6 | 26.2 | 25.3 | 78.29 | 45% | + |
| EtOAc | 15.8 | 5.3 | 7.2 | 98.6 | 18.2 | 6.08 | 77.11 | 25% | − |
| isopropanol | 15.8 | 6.1 | 16.4 | 76.8 | 24.5 | 19 | 82.3 | 8% | + |
| DCM | 18.2 | 6.3 | 6.1 | 63.9 | 20.0 | 8.9[c] | 40 | 10% | − |
| diethyl ether | 16.4 | 2.9 | 5.1 | 104.8 | 15.1 | 4.3 | 34.5 | ny | na |
| hexane | 14.9 | 0 | 0 | 131.6 | 14.9 | 1.89 | 68.73 | ny | na |

[a](δD, dispersion; δP, polarity; δH, hydrogen bonding; δ, solubility; ε, dielectric constant; $b_p$, boiling point). [b]at 295.2K. [c]at 298.0 K; ny, negligible yield; +, large amount of carbohydrate; −, trace amount of carbohydrate; na, nonanalyzed for its lower yield. Abbreviations: dimethyl sulfoxide (DMSO); *N*,*N*-dimethyl formamide (DMF), tetrahydrofuran (THF), acetone (dimethyl ketone, DMK), methanol (MeOH), ethanol (EtOH), ethyl acetate (EtOAc), and dichloromethane (DCM).

of carbohydrates (LG-TC0) and the insoluble fraction with a large amount of carbohydrate (LG-LC0). Then, LG-TC0 was divided into four fractions by sequential extraction, namely, EtOAc-soluble (LG-TC1), EtOH-soluble (LG-TC2), MeOH-soluble (LG-TC3), and residue out of LG-TC0 (LG-TC4). LG-LC0 was sequentially extracted by EtOH, MeOH, and THF to obtain fractions with a high amount of carbohydrates, namely, LG-LC1, LG-LC2, and LG-LC3. Sequential extraction by each solvent was repeated several times until an almost colorless supernatant was obtained after the last extraction. A 0.22 μm nylon membrane was used for liquid−solid separation. Each fraction solution was concentrated by rotary evaporation using a Büchi interface I-300 (50 °C, 80 rpm/min) and further dried in a vacuum oven (45 °C).

**Lignin Fractions Characterization.** Carbohydrate content by acid methanolysis: 10 mg of each sample was hydrolyzed by acid methanol (2 M HCl in methanol) at 105 °C for 3 h. Then, the solution was cooled down, neutralized by small amounts of pyridine, and dried by nitrogen flow. After that, samples were further dried in a 45 °C vacuum oven for 20 min to remove solvent thoroughly. Finally, samples were silylated overnight at room temperature by adding 150 μL of pyridine, 150 μL of HMDS (hexamethyldisilazane), and 70 μL of TMCS (trimethyl chlorosilane). The sugar content was determined by GC-FID (Perkin Elmer Autosystem XL Gas Chromatograph). The GC-FID parameters were based on previous reports: injection volume, 1 μL; injector temperature, 250 °C; split ratio, 1:30; the temperature of a dimethyl polysiloxane column (HP-1, Agilent Technologies, 25 m × 0.20 mm i.d) with a thickness of 0.11 μm was first increased from 100 to 180 °C at a rate of 4 °C/min and then increased to 290 °C at a rate of 12 °C/min; detector temperature, 300 °C; flow rate of carrier gas (hydrogen), 0.8 mL/min.[27] The collected data was processed using the PerkinElmer TotalChrom Microsoft Windows-based software package.

**Molar Mass Distribution.** Molar mass analyses were performed on a size-exclusion chromatograph equipped with multiangle light scattering detectors (SEC-MALS, DAWN 8, Wyatt technology) system with Agilent PolarGel M columns (7.5 × 300 $mm^2$). Dimethyl sulfoxide (DMSO) containing LiBr (0.05 M) was used as an eluent. The running parameters were as follows: sample concentration, 10 mg/mL in eluent solvents; injection volume, 100 μL; flow rate, 0.5 mL/min. All samples were filtered by a 0.22 μm nylon filter.

**$^{31}$P NMR and HSQC Analysis.** Nuclear magnetic resonance (NMR, Bruker 500 MHz) was used to quantify the hydroxyl group content of each lignin fraction following a previously reported procedure.[28] Mixture solvent (A) of chloromform-$d_6$ ($CDCl_3$) and pyridine at a ratio of (1:1.6, v/v) was used as a solvent to dissolve fractions with a trace carbohydrate content. Mixture solvent (A') of DMF/$CDCl_3$/pyridine (2:1:1, v/v) was used to dissolve lignin fractions with large carbohydrate content. A relaxation reagent of chromium(III) acetylacetonate ($Cr(acac)_3$) (11.4 mg/mL) and an internal standard solution of endo-*n*-hydroxy-5-norbornener-2,3-dicarboximide (e-HNDI) (0.12 M) were prepared with mixture solvent A. Each determined nuclear magnetic tube contained 20 mg of lignin fraction, 400 μL of solvent A (or A'), 100 μL of internal standard, 50 μL of relaxation reagent, and 100 μL of 2-chloro-4,4,5,5, tetramethyl-1,3,2-dioxaphospholane (TMDP). Moreover, 80 mg of lignin dissolved in 650 μL of DMSO-$d_6$ was used for the heteronuclear single quantum correlation spectrum (HSQC) determination using the same instrument.

**Elemental Composition and Lignin Content.** The element composition of C, H, and O was analyzed by a CHNS/O analyzer (Thermo Scientific FLASH 2000). The lignin content was determined by an acetyl bromide method according to the previous reports.[29] Briefly, around 3−5 mg of each fraction was dissolved into 5 mL of glacial acetic acid containing 25% (w/w) acetyl bromide. Then, 0.2 mL of 70% perchloric acid was added before the sample was heated at 70 °C in oil bath for 30 min. After cooling down, the solution was diluted in a buffer containing 10 mL of NaOH (2M) and 12 mL of glacial acetic acid. Then, each sample was diluted to 50 mL by glacial acetic acid. The lignin content was determined by UV−vis spectroscopy (UV2600, Shimadzu) at 280 nm. Milled softwood lignin was used as a reference. The lignin percentage content was calculated with the following equation.

$$\text{lignin content}\ (\%) = 100\% \times [(A_{\text{sample}} - A_{\text{blank}})/0.43\ \text{mg}^{-1}]/m_0$$

where $A_{\text{sample}}$ and $A_{\text{blank}}$ are the absorbance values at 280 nm of the sample and the blank, respectively, and $m_0$ is the mass of each lignin sample.

**Thermal Gravimetric Analysis (TGA) and Differential Scanning Calorimetry (DSC).** TGA was carried out using a STD-600 TGA analyzer from TA Instruments. The profiles were obtained using $N_2$ in a flow of 50 mL/min from room temperature to 700 °C at an increasing rate of 10 °C/min. DSC curves were collected via DSC-250 (TA Instruments). The samples were heated from 0 to 200 °C at a heating rate of 10 °C/min (isothermal hold for 1 min at 200 °C), cool down to 0 °C with a cooling rate of 20 °C/min, and then heated to 200 °C/min under a $N_2$ flow (100 mL/min). The second heating scan was to analyze the glass transition temperature.



https://doi.org/10.1021/acssuschemeng.2c04498
ACS Sustainable Chem. Eng. 2022, 10, 14588−14599

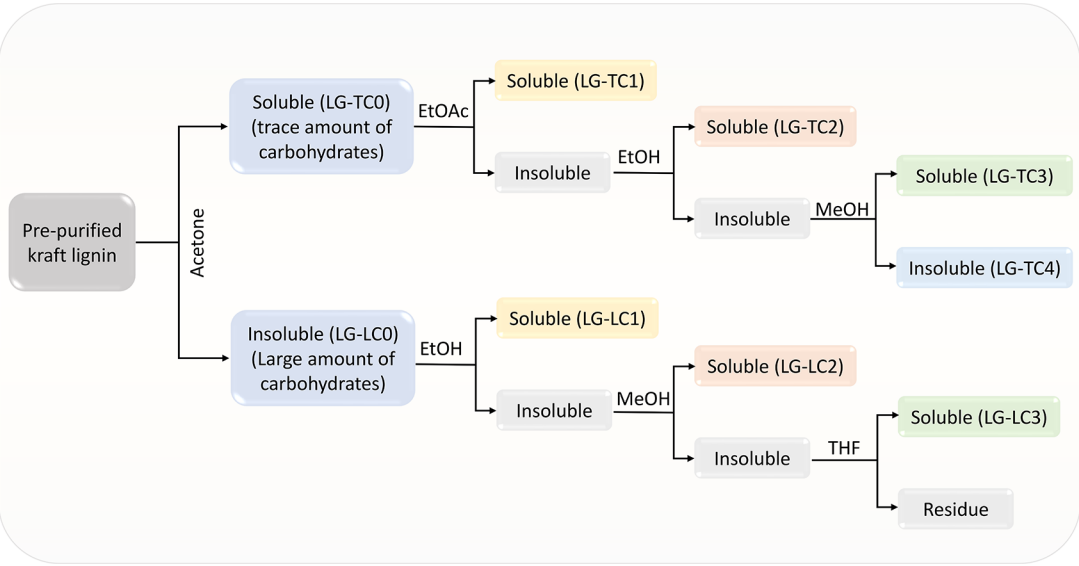


**Figure 1.** Lignin fractionation by sequential organic solvents.

**Lignin Nanoparticles Preparation and Characterization.** Two milligrams per milliliter solution of each lignin fraction was prepared using aqueous acetone (75 wt %). Nanoparticles were prepared by dropping 10 mL of water (50 mL/min) into 1 mL of lignin solution under vigorous stirring. The acetone was removed by rotary evaporation. The particle size of each fraction was determined by the differential light scattering (DLS) method (Zetasizer nano series, Malvern). In addition, transmission electron microscopy (TEM, Jeol JEM-1400 plus) was used to study the morphology of the synthesized nanoparticles.

## RESULT AND DISCUSSION

**Solvents Screening.** To preliminarily verify the hypothesis that a solvent with a higher hydrogen bonding ability would accelerate the dissolution of lignin with larger carbohydrates content, organic solvents commonly used for lignin chemistry were individually employed to extract lignin fractions. Table 1 presents the critical physicochemical parameters of solvents, the extraction yield by each solvent, and the qualitative carbohydrate content. Due to careful washing and prepurification, the prepurified kraft lignin almost could not be extracted by dimethyl ether and hexane, which are solvents with lower polarity and lower hydrogen bonding ability.[30] The fraction yield obtained by DCM can go up to 10%, but only rather weak carbohydrate signals were detected from its acid methanolysis products (Figure S1). The dissolution of the prepurified lignin in other solvents and the carbohydrate content in each of these fractions were obviously different. In short, the result of the carbohydrate content analysis in these fractions indicated that the solvents with higher a $\delta$H, such as DMSO, DMF, dioxane, THF, MeOH, EtOH, and isopropanol, are capable of isolating lignin with a certain amount of carbohydrates. In contrast, the solvents with a relatively low $\delta$H, as for DMK, EtOAc, and DCM, could only extract lignin with a trace amount of carbohydrate. These results were consistent with previous reports that lignin with a rather low carbohydrate content was extracted by the solvents with a lower hydrogen bonding ability such as ethyl acetate, DMK, DCM, and diethyl ether.[30−32] Note, as an exception, pyridine, which has even a lower hydrogen bonding ability compared to DCM, could extract lignin with large amounts of carbohydrates. One tentative explanation is that the basic solvent contributes to the ionization and solvation of the carbohydrates and thus promotes the dissolution of carbohydrate-bonded lignin.[3]

In summary, the results strongly indicated that the solvents with a higher $\delta$H ($\geq$8 in this work) could improve the solubility of lignin with carbohydrates, while it should be borne in mind that multiple factors, such as $\delta$D, $\delta$P, the molecular size of solvent, the dielectric constant, etc., also potentially influence the solubility of lignin with a trace/large carbohydrate content. These factors are not discussed in depth here since the potential influence of hydrogen bonding ability is the focus of this work.

**Solvents Selection for Sequential Extraction.** As shown by the preliminary carbohydrate content results of the fractions singly isolated by different solvents, a higher $\delta$H solvent could more likely promote the dissolution of lignin bonded with carbohydrates. Therefore, we proceeded to determine an optimal solvent sequence to separate lignin fractions with different carbohydrate contents, as well as to decrease their molar mass. For lignin fractionation by organic solvents, the following factors should be considered: the dissolution ability of lignin, safety, environmental and regulatory considerations, and the cost. Hexane, diethyl ether, dichloromethane, dioxane, and pyridine are thus not suitable solvents and are undesirable. DMSO and DMF were also excluded for their nonselectivity to lignin with/without carbohydrates. Isopropanol was not employed in further sequential extraction for its lower extraction yield from the prepurified lignin, even if carbohydrate signals were observed from the isopropanol-soluble fraction. Finally, THF, DMK, MeOH, EtOH, and EtOAc were selected as feasible alternates for lignin fractionation in this study.

DMK has been confirmed to be an excellent solvent to selectively extract abundant amounts of fractions with a trace amount of carbohydrates both in previous reports as well as in this study.[30,35,36] Since DMK could extract 67% of the lignin fraction with a trace amount of carbohydrates by single solvent extraction, we therefore chose DMK to separate the prepurified lignin into two parts: acetone-soluble with a trace amount carbohydrates (LG-TC0) and acetone-insoluble with large amounts of carbohydrates (LG-LC0), as shown in Figure 1. In


https://doi.org/10.1021/acssuschemeng.2c04498
ACS Sustainable Chem. Eng. 2022, 10, 14588−14599

a previous study,[26] we demonstrated that lignin fractions with increasing Mw could be obtained by the solvent sequence of EtOAc, EtOH, MeOH, acetone, and dioxane. Moreover, the carbohydrate signals were detected from the fraction extracted by EtOH, MeOH, and dioxane. Thus, the LG-TC0 was separated into four fractions by EtOAc (LG-TC1), EtOH (LG-TC2), MeOH (LG-TC3), and LG-TC4. In this study, the solvent screening results indicated that a similar fraction yield was obtained by THF and dioxane, the two common solvents always used in lignin chemistry. Therefore, we could infer that THF is effective as dioxane to dissolve higher Mw lignin molecular with/without carbohydrate. Besides, considering the carbohydrate content increasing in the fractions extracted by EtOH, MeOH, and THF, these solvents were employed to fractionate LG-LC0 to obtain fraction LG-LC1, LG-LC2, and LG-LC3.

**Molar Mass and Elemental Composition.** Sequential solvent fractionation is a commonly adopted strategy to narrow down the molar mass of lignin. Figure 2 records the molar mass curves of each sample, and Table 2 displays the calculated number- and weight-average molar mass (Mn, Mw), the yield, the elemental content of carbon (C), hydrogen (H), and oxygen (O), and the lignin content of each fraction. Obviously, the molar mass of LG-TC0 prior to the sequential fractionation had a broad distribution (Mw = 11080g/mol, PDI = 2.26). The molar mass increased gradually in the subsequent four fractions (LG-TC1, LG-TC2, LG-TC3, and LG-TC4) with a trace amount of carbohydrates presented. Among these fractions, the Mw of LG-TC4, up to 10 480 g/mol, suggested that the molar mass of lignin has notable influence on lignin's solubility in solvents. Similarly, the molar mass of LG-LC0 also displayed a broad distribution. Among the sequentially extracted fractions, LG-LC1 and LG-LC2 had much lower molar masses compared to LG-LC3, whose Mw was up to 63 880 g/mol.

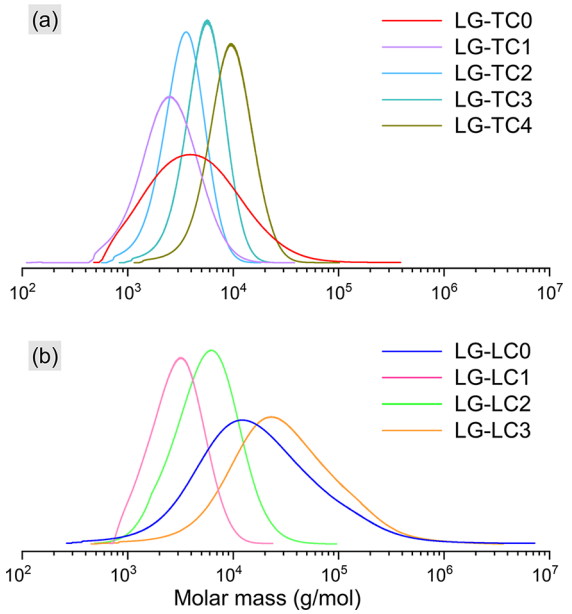


**Figure 2.** Molar mass curves of each lignin fraction, determined by SEC-MALS. (a) Lignin fractions with trace amounts of carbohydrates, and (b) lignin fractions with large amounts of carbohydrates

Softwood lignin is acknowledged as polymerized oxidation products of monolignols of coniferyl alcohol ($C_{10}H_{12}O_3$) containing 66.67% C, 26.67% O, and 6.66% H, and *p*-coumaryl alcohol ($C_9H_{10}O_2$) consisting of 72% C, 21.33% O, and 6.67% H. Moreover, it has been reported that milled wood lignin (MWL) from softwood consists of 60−63% C, 30−33% O, and 5.7−6.1% H.[37−39] Notably, kraft lignin free of carbohydrates and impurities should present a higher C/O ratio than that of MWL since lignin linkages existing in kraft lignin, such as such as phenylcoumaran, resinol, dibenzodioxin, cinnamaldehyde, and stilbene etc., have similar C and O content to coniferyl alcohol or *p*-coumaryl alcohol.[40] Thus, the elemental composition of C, H, and O could be a compelling supplement to the presence of carbohydrates as hemicellulose with 45.5% C, 48.4% O, and 6.1% H can increase the O content and conversely decrease the C content.[41] Here, the elemental composition indicated that LG-TC1, LG-TC2, LG-TC3, and LG-TC4 present higher C and lower O content than the fractions with a high carbohydrates content. In addition, the lignin contents among the trace carbohydrate content fractions were much higher than in those with a notable carbohydrate. This point was validly illustrated by the significant difference in the carbon and oxygen content among lignin fractions with trace and large carbohydrate content. It should be explained that the lignin content over 100% among the trace carbohydrate lignin fraction is reasonable. That is because a higher absorbance value of kraft lignin may be ascribed to the abundant chromophores and auxochromes groups that are originated from the formed —CH═CH— bonds conjugated

**Table 2. Calculated $M_w$, $M_n$, PDI, the Yield of Each Fraction, the Elemental Percentage Composition of Carbon (C), Hydrogen (H), and Oxygen (O), and the Lignin Content Determined by Acetyl Bromide Method[c]**

| sample | $M_n$(g/mol) | $M_w$(g/mol) | PDI | yields[a,b] (%) | C (wt%) | H (wt%) | O (wt%) | lignin content (%) |
|---|---|---|---|---|---|---|---|---|
| LG-TC0 | 4905 | 11 080 | 2.26 | 67.4 | n | n | n | n |
| LG-TC1 | 2419 | 2788 | 1.15 | 23.3 | 66.38 | 5.85 | 26.21 | 107.97 |
| LG-TC2 | 2961 | 3687 | 1.25 | 12.1 | 65.13 | 5.83 | 26.37 | 102.94 |
| LG-TC3 | 4776 | 5866 | 1.23 | 19.4 | 65.07 | 5.89 | 26.55 | 104.06 |
| LG-TC4 | 8151 | 10 480 | 1.28 | 12.5 | 66.25 | 5.91 | 26.48 | 108.29 |
| LG-LC0 | 3465 | 12 180 | 3.52 | 32.6 | n | n | n | n |
| LG-LC1 | 2412 | 3768 | 1.56 | 0.85 | 63.94 | 5.98 | 28.67 | 87.93 |
| LG-LC2 | 3794 | 6820 | 1.80 | 5.21 | 61.52 | 6.31 | 30.17 | 86.47 |
| LG-LC3 | 15 410 | 63 880 | 4.14 | 16.25 | 64.45 | 6.09 | 28.56 | 93.26 |
| residue | n | n | n | 9.85 | 58.75 | 5.81 | 34.46 | 75.65 |

[a]The yield is based on the amount of initial prepurified lignin. [b]Due to slight mass loss during the sequence extraction and collection process, the yield summary of all fractions was lower than 100%. [c]n: nondetected.



https://doi.org/10.1021/acssuschemeng.2c04498
ACS Sustainable Chem. Eng. 2022, 10, 14588−14599

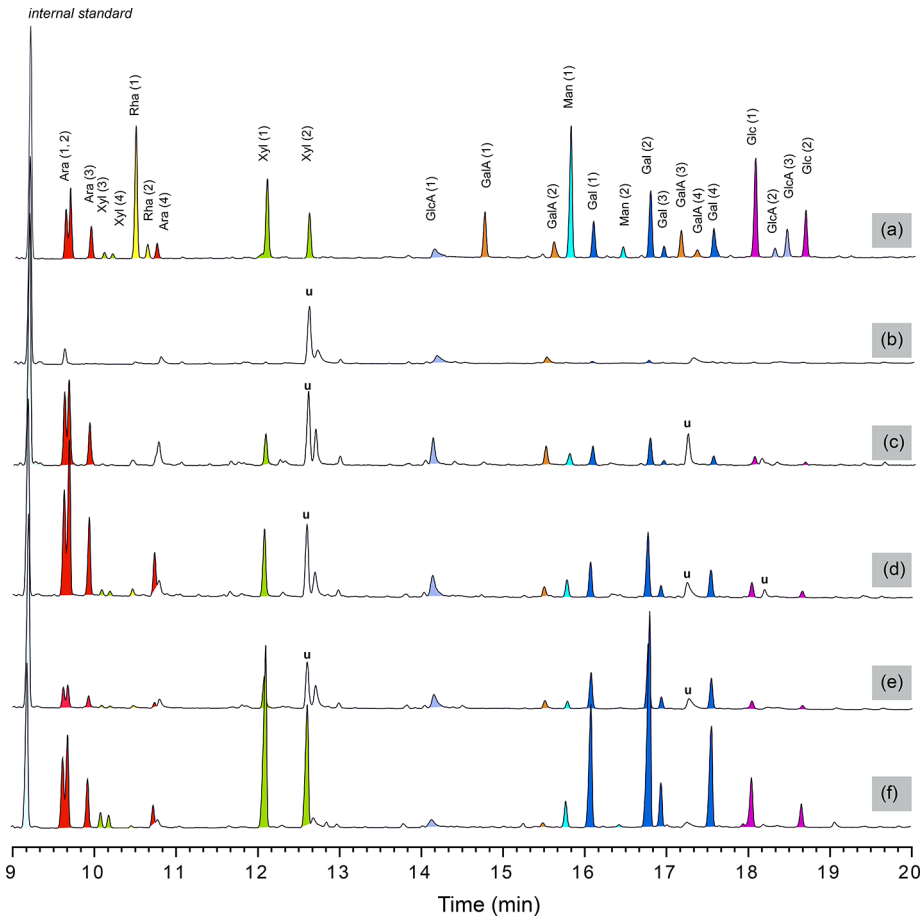


**Figure 3.** GC-FID spectra of the carbohydrate signals in each lignin fraction: (a) calibration curve; (b) acetone soluble fraction (LG-TC0); and sequentially extracted fraction out of LG-LC0, (c) LG-LC1 by EtOH, (d) LG-LC2 by MeOH, (e) LG-LC3 by THF, and (f) final residue with a large carbohydrate content. "u" peaks are uncertain substance where no obvious fragments relevant to the counterpart sugar monomer were detected by GC−MS. Ara, arabinose; Xyl, xylose; Rha, rhamnose; Gal, galactose; Glc, glucose; Man, mannose; GalA, galacturonic acid; GlcA, glucuronic acid.

**Table 3. Carbohydrate Contents in Each Lignin Fraction**[a]

| | anhydrous sugar content (mg/g) | | | | | | | | |
|---|---|---|---|---|---|---|---|---|---|
| sample | Ara | Xyl | Rha | Gal | Glc | Man | GalA | GlcA | total (mg/g) |
| LG-TC0 | n | n | n | 1.02 | n | n | 0.27 | 1.36 | 2.56 |
| LG-TC1 | 0.41 | n | n | 0.63 | n | n | 0.31 | 0.82 | 2.17 |
| LG-TC2 | 1.96 | n | n | 1.05 | 0.33 | n | 0.28 | 1.01 | 4.63 |
| LG-TC3 | 1.84 | n | n | 0.64 | 0.25 | n | 0.36 | 0.77 | 3.89 |
| LG-TC4 | 1.06 | n | n | 0.38 | 1.25 | n | 0.33 | 0.81 | 3.83 |
| LG-LC1 | 10.82 | 3.67 | 0.57 | 5.43 | 1.02 | 0.86 | 0.24 | 0.92 | 23.53 |
| LG-LC2 | 26.66 | 8.17 | 0.73 | 9.67 | 1.69 | 1.48 | 0.45 | 2.51 | 51.36 |
| LG-LC3 | 3.75 | 4.08 | 0.24 | 10.30 | 1.05 | 0.62 | 0.38 | 1.63 | 22.52 |
| Residue | 17.59 | 30.05 | 0.34 | 45.22 | 6.57 | 1.52 | 0.16 | 1.28 | 108.83 |

[a]n: noncalculated. Note: Since sugar units connected to lignin with ether bonds cannot be cleaved by acid methanolysis, the actual carbohydrate content can be higher than the results obtained by the acid methanolysis method.

with aromatic rings, the condensed structure by chalcones or *p*,*o*′-dihydroxybiphenylmethanes, and the produced quinonoid structures due to oxidative dehydrogenation during the delignification process. Moreover, the lignin content of pure kraft lignin should be higher than the milled wood lignin, which always has a minor amount of carbohydrates.

**Carbohydrate Content.** Figure 3 presents the carbohydrate chromatograms of LG-LC0, LG-LC1, LG-LC2, LG-LC3, and the residue out of LG-LC0. Table 3 contains the carbohydrate contents in each lignin fraction. The chromatogram clearly shows that only rather weak signals of monosaccharides, mainly GlcA, GalA, and Gal, were detected in LG-TC0. Moreover, there were no obvious monosaccharide signals in the fractions with trace carbohydrate content, LG-TC1, LG-TC2, LG-TC3, and LG-TC4 (Figure S2). As expected, all monosaccharide signals were detected from the fractions that were isolated from LG-LC0. However, significant differences were observed in monosaccharide types and


https://doi.org/10.1021/acssuschemeng.2c04498
ACS Sustainable Chem. Eng. 2022, 10, 14588−14599

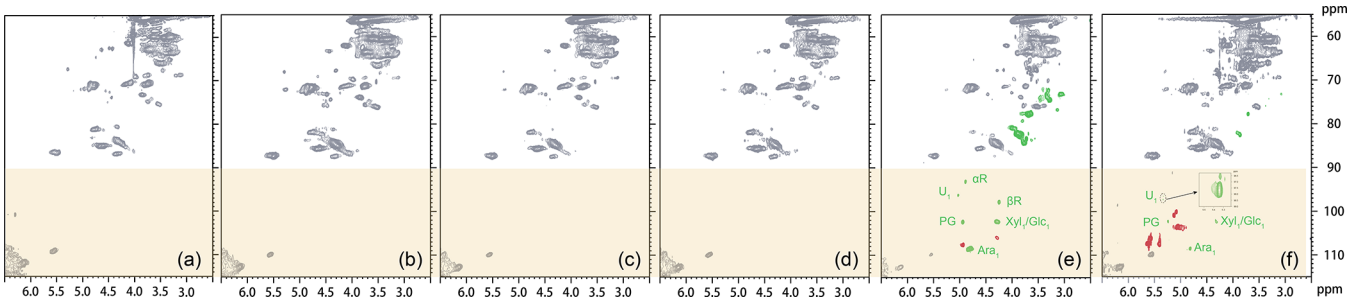


**Figure 4.** HSQC NMR result of lignin fractions in the oxygenated region: (a) LG-TC1, (b) LG-TC2, (c) LG-TC3, (d) LG-TC4, (e) LG-LC2, and (f) LG-LC3. $\alpha$R ($\delta$C/$\delta$H: 93.23/4.89 ppm) and $\beta$R ($\delta$C/$\delta$H: 97.49/4.24 ppm), $\alpha$- and $\beta$-reducing end carbohydrate units; PG, phenyl glycoside (Glc ($\delta$C/$\delta$H: 102.53/4.95 ppm); Man Gal), $U_1$ ($\delta$C/$\delta$H: 96.29/5.03 ppm), nonesterified uronic acids units; $X_1$/$Glc_1$ ($\delta$C/$\delta$H: 102.33/4.28 ppm), xylofuranoside/glucopyranoside; $Ara_1$ ($\delta$C/$\delta$H: 108.44/4.82 ppm), arabinofuranoside, and the unidentified signal (red).

**Table 4. Hydroxyl Groups Content of Each Lignin Fraction, Detected by $^{31}$P-NMR**

| | phenolic −OH (mmol/g) | | | | | | |
|---|---|---|---|---|---|---|---|
| sample | C5-substituted | guaiacyl −OH | *p*-hydroxylphenyl −OH | total phenolic −OH | aliphatic −OH (mmol/g) | carboxylic acid −COOH (mmol/g) | total −OH (mmol/g) |
| LG-TC1 | 2.08 | 1.97 | 0.21 | 4.26 | 1.68 | 0.39 | 6.33 |
| LG-TC2 | 1.79 | 1.73 | 0.19 | 3.71 | 2.27 | 0.43 | 6.41 |
| LG-TC3 | 1.97 | 1.68 | 0.21 | 3.86 | 2.23 | 0.28 | 6.37 |
| LG-TC4 | 1.86 | 1.55 | 0.22 | 3.63 | 2.04 | 0.26 | 5.93 |
| LG-LC1 | 1.78 | 1.76 | 0.19 | 3.73 | 2.68 | 0.30 | 6.71 |
| LG-LC2 | 1.72 | 1.65 | 0.16 | 3.53 | 2.63 | 0.31 | 6.47 |
| LG-LC3 | 1.65 | 1.34 | 0.15 | 3.14 | 2.80 | 0.27 | 6.21 |

content among the fractions with an obvious carbohydrate content. In LG-LC1 and LG-LC2, arabinose (Ara) is the most abundant monosaccharide. However, in LG-LC3, which was isolated by THF, the galactose (Gal) content is much higher than other kinds of monosaccharides. The final residue out of LG-LC0 shows a rich content of Gal, xylose (Xyl), Ara, and Glc. Interestingly, the distribution of these monosaccharides has a potential relationship with the molar mass of these fractions. The lower molar mass fractions, LG-LC1 and LG-LC2, have a higher pentose content. In contrast, LG-LC3 with a high molar mass is rich in galactose. Previous reports have revealed that the covalent linkages between lignin and carbohydrates can form various lignin-carbohydrate complexes (LCCs) depending on the ratio of each monosaccharide, such as a galactoglucommannan LCC, a glucan LCC, a xylan−lignin−glucomannan network LCC, a glucomannan−lignin−xylan network LCC, and so on.[42−46] Thus, it is reasonable to assume that various LCC fractions would be coprecipitated with lignin from black liquor. Moreover, Lawoko et al. reported that condensed bond discrepancies in the quantity of arabinoxylan-bound lignin and glucomannan-bound lignin can result in different lignification speeds during chemical pulping.[24] This could be one reason that the monosaccharides both in types and content showed notable differences among these carbohydrates covalently bonded lignin.

**HSQC NMR and $^{31}$P NMR Results.** HSQC NMR is an intuitive technique for the identification of the carbohydrates in lignin, which usually appears as strong cross-peaks in the oxygenated region. Figure 4 describes the HSQC NMR spectra of each lignin fraction. Due to the selectivity of acetone to the lignin fraction with a trace amount of or without carbohydrates, there are almost no obvious carbohydrate signals in the fraction. In contrast, the fractions obtained from the acetone insoluble sample reveal strong carbohydrate signals, especially at the anomeric region. Moreover, in the region of $\delta$C/$\delta$H 55−115/2.5−6.5 ppm, the LG-LC2 unfolds sharp peaks belonging to pentoses (marked in green). The results are well in line with the acid methanolysis analysis that LG-LC2 is enriched in arabinose and xylose. In LG-LC3, the siganals for hexoses are stronger than that of the pentoses, which is in good agreement with the result that the total hexose (Gal, Glc, and Man) content is higher than that of pentoses. The carbohydrate signal in LG-LC1 was not detected by HSQC due to its low yield. In turn, the acid methanolysis results and the C and O percentage composition demonstrated well that EtOH is effective in promoting the dissolution of low Mw lignin bonded with a certain amount of carbohydrates.

**$^{31}$P NMR Results.** The contents of functional hydroxyl groups in each lignin fraction were calculated based on the $^{31}$P NMR spectra by integration of the peak areas. Table 4 shows the contents of phenolic groups, aliphatic hydroxyl groups, and carboxyl groups. Overall, the total phenolic hydroxyl content varies with the total phenolic and aliphatic −OH. Among fractions with a trace amount of carbohydrates, LG-TC1 with the lowest $M_w$ has the highest content of total phenolic −OH but has the lowest content of aliphatic −OH than other fractions, which is in accordance with the general view that low $M_w$ lignin fractions always have a high concentration of phenolic hydroxyl group.[47] An increase in molar mass does not significantly change the total phenolic −OH content among LG-TC2, -TC3, and -TC4. Still, the total −OH in LG-TC2 and LG-TC3 is higher due to the higher aliphatic −OH. A probable reason is that EtOH and MeOH have strong dissolving abilities to lignin with more aliphatic −OH that may originate from side chains and even the trace amount of carbohydrates. With respect to the fractions with a larger carbohydrate content, as expected, the aliphatic −OH content increases in LG-LC1, -LC2, and -LC3. Therefore, the carbohydrates covalently bonded with lignin would contribute to the aliphatic −OH content. Moreover, the abundant


https://doi.org/10.1021/acssuschemeng.2c04498
ACS Sustainable Chem. Eng. 2022, 10, 14588−14599

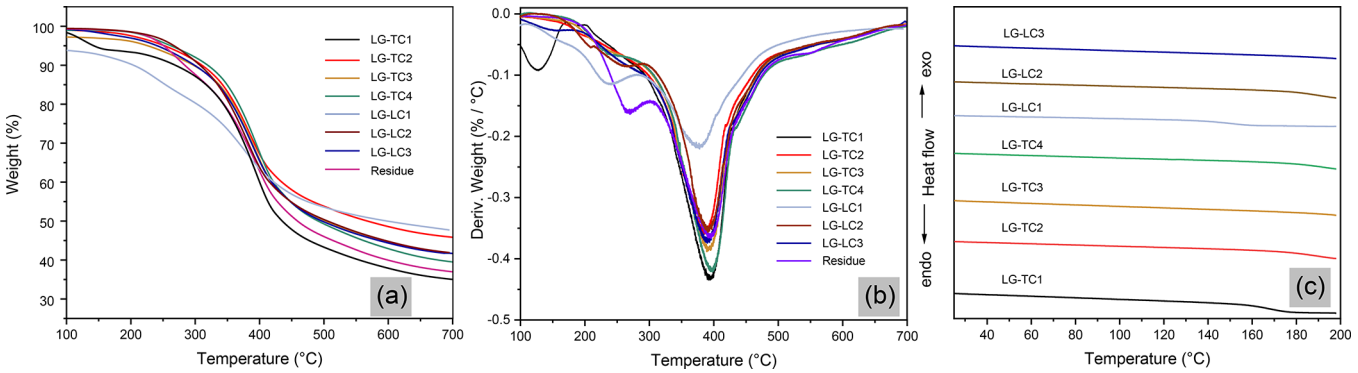


**Figure 5.** (a) TGA, (b) DTG, and (c) DSC curves of each lignin fraction at a $N_2$ atmosphere.

carbohydrates in the high $M_w$ lignin could be a feasible explanation for the pervasive phenomenon that a higher $M_w$ lignin fraction would contain a much higher content of hydroxyl groups.[15]

**Thermal Properties.** Due to the abundant aromatic backbone, lignin is moderately stable at elevated temperatures, and this significant characteristic makes lignin a popular candidate for developing lignin-based thermal copolymers, blends, and composites.[7] Therefore, it is necessary to carry out a fundamental study on the thermal degradation and DSC behavior of these lignin fractions with trace/larger amounts of carbohydrates for their potential applications.

The differences in the molar mass and carbohydrate content considerably influence the thermal properties of each lignin fraction. Among fractions with trace amount of carbohydrates, LG-TC2, LG-TC3, and LG-TC4 presented similar thermal degradation behaviors for the temperature at the mass loss of 10% ($T_{10\%}$), 50% ($T_{50\%}$), and at the maximum rate of mass loss (the peak of the derivative weight, $T_{DTGmax}$), shown in Figure 5 and Table 5. For the lowest $M_w$ LG-TC1, the $T_{10\%}$ and $T_{50\%}$ were found to decreased significantly but the $T_{DTGmax}$ stayed at the same level with the higher molar mass fractions in the range 390−400 °C. Interestingly, according to the results of elemental analysis, the C/O ratios of the fractions with trace amounts of carbohydrates were pretty close to each other; however, the char mass residue (35.02%) of LG-TC1 at 700 °C was much lower compared to those of LG-TC2 (42.58%), LG-TG3 (41.62%), and LG-TC3 (40.69%). These results suggested that LG-TC1, extracted by ethyl acetate, may contain more thermally sensitive subunits.

**Table 5. Thermal Degradation Temperatures at Mass Loss of 10% ($T_{10\%}$) and 50% ($T_{50\%}$) and Maximum Mass Loss Derivative Temperature ($T_{DTGmax}$) and Final Residue Percentage at 700 °C**[a]

| | temperature (°C) | | | | |
|---|---|---|---|---|---|
| sample | $T_{10\%}$ | $T_{50\%}$ | $T_{DTGmax}$ | $T_g$ | residue (wt %) |
| LG-TC1 | 268 | 433 | 393 | -[a] | 35.02 |
| LG-TC2 | 310 | 566 | 390 | -[a] | 44.58 |
| LG-TC3 | 300 | 501 | 392 | -[a] | 41.62 |
| LG-TC4 | 318 | 490 | 396 | -[a] | 39.58 |
| LG-LC1 | 297 | 477 | 391 | -[a] | 38.45 |
| LG-LC2 | 265 | 489 | 358 | -[a] | 38.88 |
| LG-LC3 | 298 | 495 | 388 | -[a] | 41.69 |
| residue | 283 | 398 | 394 | nd[b] | 36.23 |

[a]$T_g$ is not observed. [b]nd: nondetected.

The fractions with a larger carbohydrate content, and the final residue especially, which has the most abundant carbohydrates, exhibit obvious decomposition in two stages, a minor degradation at 220−305 °C and a major degradation at 390−400 °C, as seen in Figure 5b. Differently, LG-LC3 mainly contained lower content of hexose-based carbohydrates and did not significantly decompose at 220−305 °C. Studies have confirmed that the thermal degradation of polysaccharides from hemicellulose such as galactomannan and arabinoxylan always take place at a range of 200−280 °C.[40] Moreover, it has been reported that, due to different decomposition mechanisms, there are distinct thermal degradation discrepancies between pentose- and hexose-based polysaccharides.[48,49] Thus, the minor degradation should be ascribed to the degradation of carbohydrates in each fraction. And, this result also suggested that the differences in the types and contents of polysaccharides covalently bound with lignin may mislead on the understanding of thermal degradation behavior of pure lignin.

The glass transition temperature ($T_g$) is another important parameter for describing thermal properties of lignin. However, the $T_g$ of lignin still seems to be a controversial issue. In general, the $T_g$ of lignin was reported to be in a range of 110−150 °C, depending on the lignin types and lignin $M_w$.[50] However, it was also reported that no clear change in the DSC curve could be observed in the well-fractionated lignin.[51] In this study, DSC determination was performed to evaluate the potential $T_g$ of each fraction, and the results are shown in Figure 5c. Overall, an obvious endothermal event was only recorded in LG-TC1. However, this endothermal event cannot strongly prove that LG-TC1 has a $T_g$ temperature, because it is difficult to figure out the underlying cause for the change, as even phase transition or decomposition or both at a same time are possible. TGA combined with FTIR was used for a further analysis, and when the LG-TC1 was decomposed from room temperature to 180 °C at a same heating speed, the detected signals (90−170 °C) indicated that the endothermal peak may be caused by substance decomposition or evaporation (Figure S3). It is worth mentioning that the components removed by MTBE showed several endothermal peaks and lower thermal stability (Figure S4). However, the MTBE extractives consist of various components with lower boiling points, such as fatty acids, resin acids, and phenolic compounds relevant to lignin or lignan (Table S3), which may lead to varying $T_g$ values if mixed with lignin samples.



https://doi.org/10.1021/acssuschemeng.2c04498
ACS Sustainable Chem. Eng. 2022, 10, 14588−14599

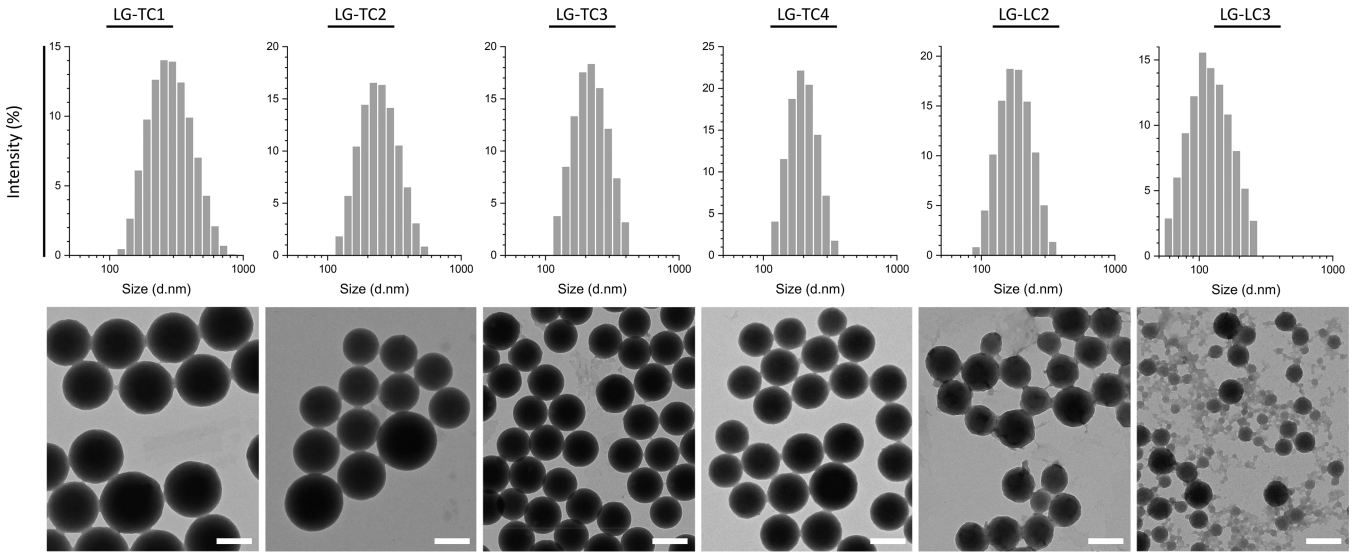


**Figure 6.** Size distribution of LG-TC1, 291 nm; LG-TC2, 254 nm; LG-TC3, 227 nm; LG-TC4, 202 nm; LG-LC2, 185 nm; LG-LC3, 130 nm that were determined by DLS (the first row). TEM images of each LGNPs in the second row. Scale bar: 200 nm.

**Influence on Lignin Nanoparticle Formation.** The fast-growing field of nanotechnology has significantly promoted the advancement of nanomaterials in various sectors such as agriculture, energy, and nanomedicine. Lignin is known as a natural aromatic polymer with an excellent ability to self-assemble into nanoparticles (LGNPs) by solvent exchange methods. Tempting application opportunities for LGNPs in various fields have stimulated extensive research on factors that influence the morphology and size distribution of LGNPs. For instance, the discrepancies in the water dropping rate,[52] stirring speed,[53] solvent for lignin dissolution,[54] initial concentration,[55] as well as the lignin properties (molar mass, functional groups content)[56] could significantly influence the physical characteristics of the resulted nanoparticles. However, few attention has been paid to the influence of the carbohydrate content on the final nanoparticles. In this work, we have successfully separated the lignin fractions according to the carbohydrate content as well as the molar mass. The particles from trace and highly carbohydrate-containing lignin fractions were prepared and characterized to understand the possible difference.

Up to now, various (aqueous) solvents, ethanol, methanol, acetone, THF, dioxane, DMSO, etc., have been applied for lignin dissolution for lignin nanoparticles preparation.[37,57−61] However, acetone, especially its aqueous solution, has been demonstrated to be an excellent solvent due to it being more environmentally friendly and having an increased ability to dissolve lignin and a unique ability to form uniform LGNPs by nanoprecipitation.[62] Thus, in this study, aqueous acetone (75 wt %) was used as a solvent for the higher carbohydrate content fractions that cannot be dissolved in anhydrous acetone.

As shown in Figure 6, the size of the resulting nanoparticles was inversely proportional to the $M_w$. Lignin is an amphiphilic macromolecule due to the abundant presence of phenolic and hydroxyl groups and its benzene structure. During the self-assembly process, the hydrophobic parts of lignin aggregates form a core structure due to the desolvation of the hydrophobic parts by the progressive addition of the water. Moreover, the hydrophobic aggregation can be stabilized by a corona that was formed by the hydrophilic groups. In general, the core size of a polymer spherical particles can be regulated by the average number of polymer chains in an aggregate.[63] Larger lignin polymers may result in smaller aggregates to form a stable core domain, which presented as a smaller total interfacial area and lower total interfacial energy between the core and the antisolvent.[63] In contrast, the smaller $M_w$ fraction may increase the average number of lignin chains in an aggregate, which consequently increases the core size and yields larger spherical LNPs.[63] Thus, the size discrepancy among these nanoparticles could be observed by DLS and TEM.

In addition, the TEM images also revealed distinct differences in morphology. LGNPs originating from fractions with a trace carbohydrate content exhibited a smoother surface than those with a larger carbohydrate content, which give a more cross-like surface structures surface and even irregular aggregates that are observed in LG-LC3. It is well-known that the morphology of amphiphilic copolymer nanoparticles can be changed by factors such as the relative ratio of the hydrophobic to hydrophilic block length and the solvent interaction strength between solute and solvent. Compared to fractions with a trace carbohydrate content, the presence of abundant carbohydrates covalently bonded with lignin undoubtedly could increase the hydrophilicity of lignin, and this could be a reason that it was aqueous acetone rather than anhydrous acetone that showed better solubility to LG-LC2 and LG-LC3. As a result, the nanoparticle morphologies were different due to the potential variation in interactions between the solvent and lignin fraction during the self-assembly process of nanoparticles.

## DISCUSSION

Without fine separation, industrial softwood kraft lignin would be a highly complex mixture. In addition to the unfavorable impurities such as various wood extractives and chemical residues, the mixture always contains lignin of varying molar masses due to structural changes, such as cleavage of $\alpha$-O-4 and $\beta$-O-4 linkages leading to the formation of low $M_w$ lignin and condensation reactions between lignin molecules can result in high $M_w$ lignin. Besides, LCCs coexisting in industrial lignin may vary randomly in type, molar mass, and even total


https://doi.org/10.1021/acssuschemeng.2c04498
ACS Sustainable Chem. Eng. 2022, 10, 14588−14599

content depending on wood resources, delignification processes, and methods used for lignin enrichment, which whereafter can influence lignin in unpredictable ways. Therefore, the separation of lignin and LCCs from industrial lignin is necessary when studying the solvent solubility to lignin, the structural properties of lignin, and even lignin applications.

Since the late 20th century, increasing research efforts have been devoted to lignin fractionation to obtain more structurally homogeneous fractions and to support the development of higher value-added lignin-based products. However, the initial physicochemical characteristics of the raw lignin to be fractionated frequently vary, depending on the biomass sources (softwood, hardwood, or grasses), industrial delignification processes, and the method to lignin enrichment. Therefore, numerous methods for fractionation have been proposed depending on the type of technical lignin, as well as the objectives of the applications.[64]

The prevalent approaches for the fractionation of industrial lignin are based on two main categories, solvent- and membrane-mediated, and have been elaborately summarized in a previous review.[15] Membrane filtration is a successful method to obtain lignin with a specific molar mass, in accordance with the membrane cut-offs. However, lignin fractions free of carbohydrate may not be achieved when LCC with a high PDI is mixed in the initial lignin sample.[65] Solvent fractionation using a single solvent, a mixture of solvents, or aqueous organic solvents is a simple procedure to extract a lignin component. Similarly, LCC can also be extracted from the raw lignin sample by solvents with stronger hydrogen bonding abilities, such as ethanol, methanol, THF, and dioxane, as has demonstrated in this study and previous reports. For example, carbohydrate signals were always present in the fractions that were extracted by methanol, ethanol, dioxane, and some solvent−water cosystems.[66] Besides, the physicochemical properties of lignin fractions obtained by single solvent extraction can vary significantly due to the variable raw lignin source. In addition, sequential solvent extraction, which uses solvents with different solvent parameters to extract lignin by the precipitation of redissolved lignin in a gradient manner, has been proven an effective strategy to obtain more homogeneous lignin samples. Up to date, solvent sequences, for instance, DCM → MeOH,[67] DCM → isopropanol → MeOH → mixture of MeOH/DCM,[68] ethyl acetate → isopropanol → EtOH → MeOH → actone,[20,26] and isopropanol → EtOH → MeOH,[69] have been used to decrease the heterogeneity of lignin. And, the existence of carbohydrates in fractions extracted by isopropanol, EtOH, and MeOH has been confirmed. As stated in the study, the varying amounts of carbohydrates in the lignin had a notable impact on lignin dissolution in solvents, thermal degradation, and even on the formation of lignin nanoparticles. Therefore, it is necessary to remove the coexisting LCC in lignin fractionation and valorization since lignin both from sulfite and kraft pulping usually contains various lignin−carbohydrates complexes.[70,71]

## CONCLUSION

In conclusion, lignin fractions with trace (almost carbohydrate free) and large amounts of carbohydrates were successfully separated from industrial softwood Kraft lignin based on their differences in solubility by solvents with various hydrogen bonding capacities. The characterization indicted that a fraction with a high carbohydrate content could result in two stages of thermal decomposition occurring due to the relative lower thermal stability of carbohydrate. Besides, the presence of carbohydrates residue was demonstrated to have a great effect on the morphology of lignin nanoparticles prepared by the solvent shift method. Given that different carbohydrate contents have a significant effect on the physical and chemical properties of lignin and consequently may have an impact on lignin's application potential in different fields, we suggest that the role of carbohydrates covalently bonded with lignin deserves more research.

## ASSOCIATED CONTENT

### Supporting Information

The Supporting Information is available free of charge at https://pubs.acs.org/doi/10.1021/acssuschemeng.2c04498.

Figures of GC/FID chromatography spectra of the carbohydrate signals, TGA-FTIR spectra of LG-TC1, and TGA and DSC curves of MTBE extracted substances and table of melting and boiling point of different extractives extracted by MTBE (PDF)

## AUTHOR INFORMATION


### Corresponding Author

**Chunlin Xu** − *Laboratory of Natural Materials Technology, Åbo Akademi University, Turku FI-20500, Turku, Finland;* orcid.org/0000-0003-1860-9669; Email: chunlin.xu@abo.fi

### Authors

**Rui Liu** − *Laboratory of Natural Materials Technology, Åbo Akademi University, Turku FI-20500, Turku, Finland*

**Annika Smeds** − *Laboratory of Natural Materials Technology, Åbo Akademi University, Turku FI-20500, Turku, Finland*

**Teija Tirri** − *Laboratory of Natural Materials Technology, Åbo Akademi University, Turku FI-20500, Turku, Finland*

**Hongbo Zhang** − *Pharmaceutical Sciences Laboratory, Åbo Akademi University, Turku FI-20500, Turku, Finland; Turku Bioscience Center, University of Turku and Åbo Akademi University, Turku FI-20500, Turku, Finland;* orcid.org/0000-0002-1071-4416

**Stefan Willför** − *Laboratory of Natural Materials Technology, Åbo Akademi University, Turku FI-20500, Turku, Finland*

Complete contact information is available at: https://pubs.acs.org/10.1021/acssuschemeng.2c04498


### Author Contributions

R.L. carried out the investigation, experiments, data analysis and wrote the original draft. A.S. assisted in the GC analysis. T.T. assisted in the TG and DSC experiments. C.X. supervised and conceptualized this study. H.Z. cosupervised the work, while S.W. read through and commented on the manuscript.

### Notes

The authors declare no competing financial interest.

## ACKNOWLEDGMENTS

R.L. thanks Andrey Pranovich, and Jarl Hemming, who helped greatly in the GC-FID analysis, lignin content analysis, and carbohydrate content determination, respectively. China Scholar Council (201908120132) and the Doctoral Programme in Chemical and Process Engineering at Åbo Akademi University (ÅAU), and Business Finland Project (43674/31/2020) are thanked for financial support. This work is also part

of the activities within the Johan Gadolin Process Chemistry Centre (PCC) at ÅAU. The authors thank the Electron Microscopy Laboratory, Institute of Biomedicine, University of Turku, and Biocenter Finland.

## REFERENCES

(1) Ragauskas, A. J.; Beckham, G. T.; Biddy, M. J.; Chandra, R.; Chen, F.; Davis, M. F.; Davison, B. H.; Dixon, R. A.; Gilna, P.; Keller, M.; Langan, P.; Naskar, A. K.; Saddler, J. N.; Tschaplinski, T. J.; Tuskan, G. A.; Wyman, C. E. Lignin valorization: improving lignin processing in the biorefinery. *Science* **2014**, *344* (6185), 1246843.

(2) Vanholme, R.; Demedts, B.; Morreel, K.; Ralph, J.; Boerjan, W. Lignin biosynthesis and structure. *Plant Physiol* **2010**, *153* (3), 895–905.

(3) Schuerch, C. The Solvent Properties of Liquids and Their Relation to the Solubility, Swelling, Isolation and Fractionation of Lignin. *J. Am. Chem. Soc.* **1952**, *74* (20), 5061–5067.

(4) Upton, B. M.; Kasko, A. M. Strategies for the Conversion of Lignin to High-Value Polymeric Materials: Review and Perspective. *Chem. Rev.* **2016**, *116* (4), 2275–306.

(5) Wang, X.; Arai, M.; Wu, Q.; Zhang, C.; Zhao, F. Hydrodeoxygenation of lignin-derived phenolics – a review on the active sites of supported metal catalysts. *Green Chem.* **2020**, *22* (23), 8140–8168.

(6) Liu, H. L.; Chung, H. Y. Lignin-Based Polymers via Graft Copolymerization. *J. Polym. Sci. Pol Chem.* **2017**, *55* (21), 3515–3528.

(7) Sen, S.; Patil, S.; Argyropoulos, D. S. Thermal properties of lignin in copolymers, blends, and composites: a review. *Green Chem.* **2015**, *17* (11), 4862–4887.

(8) Gan, D.; Xing, W.; Jiang, L.; Fang, J.; Zhao, C.; Ren, F.; Fang, L.; Wang, K.; Lu, X. Plant-inspired adhesive and tough hydrogel based on Ag-Lignin nanoparticles-triggered dynamic redox catechol chemistry. *Nat. Commun.* **2019**, *10* (1), 1487.

(9) Richter, A. P.; Brown, J. S.; Bharti, B.; Wang, A.; Gangwal, S.; Houck, K.; Cohen Hubal, E. A.; Paunov, V. N.; Stoyanov, S. D.; Velev, O. D. An environmentally benign antimicrobial nanoparticle based on a silver-infused lignin core. *Nat. Nanotechnol* **2015**, *10* (9), 817–23.

(10) Figueiredo, P.; Lintinen, K.; Kiriazis, A.; Hynninen, V.; Liu, Z.; Bauleth-Ramos, T.; Rahikkala, A.; Correia, A.; Kohout, T.; Sarmento, B.; Yli-Kauhaluoma, J.; Hirvonen, J.; Ikkala, O.; Kostiainen, M. A.; Santos, H. A. In vitro evaluation of biodegradable lignin-based nanoparticles for drug delivery and enhanced antiproliferation effect in cancer cells. *Biomaterials* **2017**, *121*, 97–108.

(11) Figueiredo, P.; Sipponen, M. H.; Lintinen, K.; Correia, A.; Kiriazis, A.; Yli-Kauhaluoma, J.; Osterberg, M.; George, A.; Hirvonen, J.; Kostiainen, M. A.; Santos, H. A. Preparation and Characterization of Dentin Phosphophoryn-Derived Peptide-Functionalized Lignin Nanoparticles for Enhanced Cellular Uptake. *Small* **2019**, *15* (24), No. 1901427.

(12) Liang, R.; Zhao, J.; Li, B.; Cai, P.; Loh, X. J.; Xu, C.; Chen, P.; Kai, D.; Zheng, L. Implantable and degradable antioxidant poly-(epsilon-caprolactone)-lignin nanofiber membrane for effective osteoarthritis treatment. *Biomaterials* **2020**, *230*, 119601.

(13) Reesi, F.; Minaiyan, M.; Taheri, A. A novel lignin-based nanofibrous dressing containing arginine for wound-healing applications. *Drug Deliv Transl Res.* **2018**, *8* (1), 111–122.

(14) Wang, D.; Jang, J.; Kim, K.; Kim, J.; Park, C. B. "Tree to Bone": Lignin/Polycaprolactone Nanofibers for Hydroxyapatite Biomineralization. *Biomacromolecules* **2019**, *20* (7), 2684–2693.

(15) Gigli, M.; Crestini, C. Fractionation of industrial lignins: opportunities and challenges. *Green Chem.* **2020**, *22* (15), 4722–4746.

(16) Boeriu, C. G.; Fitigau, F. I.; Gosselink, R. J. A.; Frissen, A. E.; Stoutjesdijk, J.; Peter, F. Fractionation of five technical lignins by selective extraction in green solvents and characterisation of isolated fractions. *Ind. Crop Prod* **2014**, *62*, 481–490.

(17) Wang, Y. Y.; Li, M.; Wyman, C. E.; Cai, C. M.; Ragauskas, A. J. Fast Fractionation of Technical Lignins by Organic Cosolvents. *ACS Sustainable Chem. Eng.* **2018**, *6* (5), 6064–6072.

(18) Zheng, L.; Lu, G.; Pei, W.; Yan, W.; Li, Y.; Zhang, L.; Huang, C.; Jiang, Q. Understanding the relationship between the structural properties of lignin and their biological activities. *Int. J. Biol. Macromol.* **2021**, *190*, 291–300.

(19) Ribeiro, W. C. O.; Lobosco, V.; Martinez, P. F. M. Solubility Parameters Analysis of Eucalyptus urograndis Kraft Lignin. *Bioresources* **2020**, *15* (4), 8577–8600.

(20) Duval, A.; Vilaplana, F.; Crestini, C.; Lawoko, M. Solvent screening for the fractionation of industrial kraft lignin. *Holzforschung* **2016**, *70* (1), 11–20.

(21) Thring, R. W.; Vanderlaan, M. N.; Griffin, S. L. Fractionation Of Alcell® Lignin By Sequential Solvent Extraction. *J. Wood Chem. Technol.* **1996**, *16* (2), 139–154.

(22) Sadeghifar, H.; Ragauskas, A. Perspective on Technical Lignin Fractionation. *ACS Sustainable Chem. Eng.* **2020**, *8* (22), 8086–8101.

(23) Hansen, C. M.*Hansen solubility parameters: a user's handbook*; CRC Press, 2007.

(24) Lawoko, M.; Henriksson, G.; Gellerstedt, G. Structural differences between the lignin-carbohydrate complexes present in wood and in chemical pulps. *Biomacromolecules* **2005**, *6* (6), 3467–73.

(25) Tarasov, D.; Leitch, M.; Fatehi, P. Lignin-carbohydrate complexes: properties, applications, analyses, and methods of extraction: a review. *Biotechnol Biofuels* **2018**, *11* (5), 269.

(26) Liu, R.; Smeds, A.; Wang, L. Y.; Pranovich, A.; Hemming, J.; Willfor, S.; Zhang, H. B.; Xu, C. L. Fractionation of Lignin with Decreased Heterogeneity: Based on a Detailed Characteristics Study of Sequentially Extracted Softwood Kraft Lignin. *ACS Sustainable Chem. Eng.* **2021**, *9* (41), 13862–13873.

(27) Willför, S.; Pranovich, A.; Tamminen, T.; Puls, J.; Laine, C.; Suurnäkki, A.; Saake, B.; Uotila, K.; Simolin, H.; Hemming, J.; Holmbom, B. Carbohydrate analysis of plant materials with uronic acid-containing polysaccharides–A comparison between different hydrolysis and subsequent chromatographic analytical techniques. *Ind. Crop Prod* **2009**, *29* (2–3), 571–580.

(28) Lagerquist, L.; Rahkila, J.; Eklund, P. Utilization of 31P PULCON for Quantitative Hydroxyl Group Determination in Lignin by NMR Spectroscopy. *ACS Sustainable Chem. Eng.* **2019**, *7* (9), 9002–9006.

(29) Korpinen, R.; Kallioinen, M.; Hemming, J.; Pranovich, A.; Manttari, M.; Willfor, S. Comparative evaluation of various lignin determination methods on hemicellulose-rich fractions of spruce and birch obtained by pressurized hot-water extraction (PHWE) and subsequent ultrafiltration (UF). *Holzforschung* **2014**, *68* (8), 971–979.

(30) Jaaskelainen, A.-S.; Keyrilainen, P. W.; Liitia, T.; Tamminen, T. Carbohydrate-free and highly soluble softwood kraft lignin fractions by aqueous acetone evaporation fractionation. *Nord Pulp Pap Res. J.* **2017**, *32* (4), 485–492.

(31) An, L.; Wang, G.; Jia, H.; Liu, C.; Sui, W.; Si, C. Fractionation of enzymatic hydrolysis lignin by sequential extraction for enhancing antioxidant performance. *Int. J. Biol. Macromol.* **2017**, *99*, 674–681.

(32) Zhao, C. K.; Hu, Z. H.; Shi, L. L.; Wang, C.; Yue, F. X.; Li, S. X.; Zhang, H.; Lu, F. C. Profiling of the formation of lignin-derived monomers and dimers from Eucalyptus alkali lignin. *Green Chem.* **2020**, *22* (21), 7366–7375.

(33) Barton, A. F.*CRC handbook of solubility parameters and other cohesion parameters*, 2nd ed.; CRC Press, 2017.

(34) Lide, D. R.*CRC handbook of chemistry and physics*; CRC Press, 2004; Vol. 85.

(35) Ebrahimi Majdar, R.; Ghasemian, A.; Resalati, H.; Saraeian, A.; Crestini, C.; Lange, H. Facile Isolation of LCC-Fraction from Organosolv Lignin by Simple Soxhlet Extraction. *Polymers (Basel)* **2019**, *11* (2), 225.

(36) Cui, C. Z.; Sun, R. K.; Argyropoulos, D. S. Fractional Precipitation of Softwood Kraft Lignin: Isolation of Narrow Fractions



https://doi.org/10.1021/acssuschemeng.2c04498
*ACS Sustainable Chem. Eng.* 2022, 10, 14588–14599

Common to a Variety of Lignins. *ACS Sustainable Chem. Eng.* **2014**, *2* (4), 959−968.
(37) Jin, L.; Schultz, T. P.; Nicholas, D. D. Structural Characterization of Brown-rotted Lignin. *Holzforschung* **1990**, *44* (2), 133−138.
(38) Argyropoulos, D. S.; Bolker, H. I.; Heitner, C.; Archipov, Y. 31P NMR Spectroscopy in Wood Chemistry Part V. Qualitative Analysis of Lignin Functional Groups. *J. Wood Chem. Technol.* **1993**, *13* (2), 187−212.
(39) Lindner, A.; Wegener, G. Characterization of Lignins from Organosolv Pulping According to the Organocell Process Part 1. Elemental Analysis, Nonlignin Portions and Functional Groups. *J. Wood Chem. Technol.* **1988**, *8* (3), 323−340.
(40) Lancefield, C. S.; Wienk, H. L. J.; Boelens, R.; Weckhuysen, B. M.; Bruijnincx, P. C. A. Identification of a diagnostic structural motif reveals a new reaction intermediate and condensation pathway in kraft lignin formation. *Chem. Sci.* **2018**, *9* (30), 6348−6360.
(41) Demirbaş, A. Estimating of Structural Composition of Wood and Non-Wood Biomass Samples. *Energ Source* **2005**, *27* (8), 761−767.
(42) Lawoko, M.; Henriksson, G.; Gellerstedt, G. Characterisation of lignin-carbohydrate complexes (LCCs) of spruce wood (Picea abies L.) isolated with two methods. *Holzforschung* **2006**, *60* (2), 156−161.
(43) Du, X.; Perez-Boada, M.; Fernandez, C.; Rencoret, J.; del Rio, J. C.; Jimenez-Barbero, J.; Li, J.; Gutierrez, A.; Martinez, A. T. Analysis of lignin-carbohydrate and lignin-lignin linkages after hydrolase treatment of xylan-lignin, glucomannan-lignin and glucan-lignin complexes from spruce wood. *Planta* **2014**, *239* (5), 1079−90.
(44) Balakshin, M.; Capanema, E.; Gracz, H.; Chang, H. M.; Jameel, H. Quantification of lignin-carbohydrate linkages with high-resolution NMR spectroscopy. *Planta* **2011**, *233* (6), 1097−110.
(45) Miyagawa, Y.; Tobimatsu, Y.; Lam, P. Y.; Mizukami, T.; Sakurai, S.; Kamitakahara, H.; Takano, T. Possible mechanisms for the generation of phenyl glycoside-type lignin-carbohydrate linkages in lignification with monolignol glucosides. *Plant J.* **2020**, *104* (1), 156−170.
(46) Yuan, T. Q.; Sun, S. N.; Xu, F.; Sun, R. C. Characterization of lignin structures and lignin-carbohydrate complex (LCC) linkages by quantitative 13C and 2D HSQC NMR spectroscopy. *J. Agric. Food Chem.* **2011**, *59* (19), 10604−14.
(47) Araujo, L. C. P.; Yamaji, F. M.; Lima, V. H.; Botaro, V. R. Kraft lignin fractionation by organic solvents: Correlation between molar mass and higher heating value. *Bioresour. Technol.* **2020**, *314*, 123757.
(48) Akbar, J.; Iqbal, M. S.; Massey, S.; Masih, R. Kinetics and mechanism of thermal degradation of pentose- and hexose-based carbohydrate polymers. *Carbohydr. Polym.* **2012**, *90* (3), 1386−93.
(49) Werner, K.; Pommer, L.; Brostrom, M. Thermal decomposition of hemicelluloses. *J. Anal Appl. Pyrol* **2014**, *110*, 130−137.
(50) Calvo-Flores, F. G.; Dobado, J. A.; Isac-García, J.; Martín-Martínez, F. J.*Lignin and lignans as renewable raw materials: chemistry, technology and applications*; Wiley, 2015.
(51) Sun, R. C.; Tomkinson, J.; Jones, G. L. Fractional characterization of ash-AQ lignin by successive extraction with organic solvents from oil palm EFB fibre. *Polym. Degrad. Stab.* **2000**, *68* (1), 111−119.
(52) Li, H.; Deng, Y. H.; Liu, B.; Ren, Y.; Liang, J. Q.; Qian, Y.; Qiu, X. Q.; Li, C. L.; Zheng, D. F. Preparation of Nanocapsules via the Self-Assembly of Kraft Lignin: A Totally Green Process with Renewable Resources. *ACS Sustainable Chem. Eng.* **2016**, *4* (4), 1946−1953.
(53) Xiong, F. Q.; Han, Y. M.; Wang, S. Q.; Li, G. Y.; Qin, T. F.; Chen, Y.; Chu, F. X. Preparation and formation mechanism of size-controlled lignin nanospheres by self-assembly. *Ind. Crop Prod* **2017**, *100*, 146−152.
(54) Lievonen, M.; Valle-Delgado, J. J.; Mattinen, M. L.; Hult, E. L.; Lintinen, K.; Kostiainen, M. A.; Paananen, A.; Szilvay, G. R.; Setala, H.; Osterberg, M. A simple process for lignin nanoparticle preparation. *Green Chem.* **2016**, *18* (5), 1416−1422.
(55) Zwilling, J. D.; Jiang, X.; Zambrano, F.; Venditti, R. A.; Jameel, H.; Velev, O. D.; Rojas, O. J.; Gonzalez, R. Understanding lignin micro- and nanoparticle nucleation and growth in aqueous suspensions by solvent fractionation. *Green Chem.* **2021**, *23* (2), 1001−1012.
(56) Ma, M.; Dai, L.; Si, C.; Hui, L.; Liu, Z.; Ni, Y. A Facile Preparation of Super Long-Term Stable Lignin Nanoparticles from Black Liquor. *ChemSusChem* **2019**, *12*, 5239.
(57) Sipponen, M. H.; Lange, H.; Ago, M.; Crestini, C. Understanding Lignin Aggregation Processes. A Case Study: Budesonide Entrapment and Stimuli Controlled Release from Lignin Nanoparticles. *ACS Sustain Chem. Eng.* **2018**, *6* (7), 9342−9351.
(58) Dai, L.; Li, Y. T.; Kong, F. G.; Liu, K. F.; Si, C. L.; Ni, Y. H. Lignin-Based Nanoparticles Stabilized Pickering Emulsion for Stability Improvement and Thermal-Controlled Release of trans-Resveratrol. *ACS Sustainable Chem. Eng.* **2019**, *7* (15), 13497−13504.
(59) Pylypchuk, I. V.; Lindén, P. r. A.; Lindström, M. E.; Sevastyanova, O. New insight into the surface structure of lignin nanoparticles revealed by 1H liquid-state NMR spectroscopy. *ACS Sustainable Chem. Eng.* **2020**, *8* (36), 13805−13812.
(60) Li, H.; Deng, Y. H.; Wu, H. S.; Ren, Y.; Qiu, X. Q.; Zheng, D. F.; Li, C. L. Self-assembly of kraft lignin into nanospheres in dioxane-water mixtures. *Holzforschung* **2016**, *70* (8), 725−731.
(61) Mishra, P. K.; Ekielski, A. A Simple Method to Synthesize Lignin Nanoparticles. *Colloids and Interfaces* **2019**, *3* (2), 52.
(62) Zou, T.*Lignin Nanoparticles: Understanding of Their Properties and Modifications for Versatile Applications*. PhD Dissertation, Aalto University, Finland, 2021.
(63) Mai, Y.; Eisenberg, A. Self-assembly of block copolymers. *Chem. Soc. Rev.* **2012**, *41* (18), 5969−85.
(64) Rodrigues, J. S.; Lima, V.; Araújo, L. C. P.; Botaro, V. R. Lignin Fractionation Methods: Can. Lignin Fractions Be Separated in a True Industrial Process? *Ind. Eng. Chem. Res.* **2021**, *60* (30), 10863−10881.
(65) Toledano, A.; Serrano, L.; Garcia, A.; Mondragon, I.; Labidi, J. Comparative study of lignin fractionation by ultrafiltration and selective precipitation. *Chem. Eng. J.* **2010**, *157* (1), 93−99.
(66) Zhang, H.; Bai, Y. C.; Yu, B. M.; Liu, X. X.; Chen, F. G. A practicable process for lignin color reduction: fractionation of lignin using methanol/water as a solvent. *Green Chem.* **2017**, *19* (21), 5152−5162.
(67) Mörck, R.; Reimann, A.; Kringstad, K. P. Fractionation of Kraft Lignin by Successive Extraction with Organic Solvents. III. Fractionation of Kraft Lignin from Birch. *Holzforschung* **1988**, *42* (2), 111−116.
(68) Gosselink, R. J. A.; van Dam, J. E. G.; de Jong, E.; Scott, E. L.; Sanders, J. P. M.; Li, J. E. B.; Gellerstedt, G. Fractionation, analysis, and PCA modeling of properties of four technical lignins for prediction of their application potential in binders. *Holzforschung* **2010**, *64* (2), 193−200.
(69) Wang, L.; Lagerquist, L.; Zhang, Y.; Koppolu, R.; Tirri, T.; Sulaeva, I.; Schoultz, S. v.; Vahasalo, L.; Pranovich, A.; Rosenau, T.; Eklund, P. C.; Willfor, S.; Xu, C.; Wang, X. Tailored Thermosetting Wood Adhesive Based on Well-Defined Hardwood Lignin Fractions. *ACS Sustainable Chem. Eng.* **2020**, *8* (35), 13517−13526.
(70) Lawoko, M.; Henriksson, G.; Gellerstedt, G. Characterization of lignin-carbohydrate complexes from spruce sulfite pulp. *Holzforschung* **2006**, *60* (2), 162−165.
(71) Lawoko, M.; Berggren, R.; Berthold, F.; Henriksson, G.; Gellerstedt, G. Changes in the lignin-carbohydrate complex in softwood kraft pulp during kraft and oxygen delignification. *Holzforschung* **2004**, *58* (6), 603−610.


https://doi.org/10.1021/acssuschemeng.2c04498
*ACS Sustainable Chem. Eng.* 2022, 10, 14588−14599